

# INFLUENCE OF THE CHORD AXIAL LOAD ON THE RESISTANCE OF RHS “T” JOINTS WITH AXIALLY LOADED BRACES – A PARAMETRIC STUDY

R. M. M. P. de Matos<sup>1</sup>, L. F. Costa-Neves<sup>2\*</sup>, L. R. O. de Lima<sup>3</sup>, J. G. Santos da Silva<sup>4</sup>,  
and P. C. G. da S. Vellasco<sup>3</sup>

1: Civil Engineering Department  
University of Coimbra – Pólo II - Rua Luís Reis Santos, Coimbra  
e-mail: ruimatos@dec.uc.pt

2: ISISE, Civil Engineering Department  
University of Coimbra – Pólo II - Rua Luís Reis Santos, Coimbra  
e-mail: luis@dec.uc.pt

3: Structural Engineering Department  
Faculty of Engineering - State University of Rio de Janeiro  
e-mail: lucianolima@uerj.br; vellasco@uerj.br

4: Mechanical Engineering Department  
Faculty of Engineering - State University of Rio de Janeiro  
e-mails: jgss@uerj.br

## Abstract

The intensive worldwide use of rectangular hollow sections (RHS) structural elements, mainly due to its associated aesthetical and structural advantages, led designers to be focused on the technologic and design aspects of these structures. Consequently, the accuracy of the adopted design methods is of major importance both under the economical and safety points of view.

Recent studies of connections in RHS structures pointed out for further research needs, especially for some particular geometries. This is particularly significant when the failure mode changes and the prediction of the failure load may be unsafe or uneconomical.

In this paper a numerical based parametric study performed for the analysis of a “T” connection configuration where both the chord and the brace are made of RHS sections is presented.

The connection was submitted to an incremental tension axial load in the brace up to failure while the chord was submitted to different levels of constant axial load, in tension or in compression. This task was repeated for different brace to chord width ratios and chord thicknesses, keeping the material properties constant.

A critical analysis of the results focusing on the influence of the considered parameters for the connection behaviour is presented, with an emphasis on its resistance, elastic stiffness and membrane stiffness. In addition, the numerical results for the resistance of the connection are compared to deformation limits proposed in the literature to assess the connection resistance, and to the plasticity based results from Eurocode 3.

**Keywords:** Steel structures, tubular joints, nonlinear analysis, finite element method.

---

\* Corresponding Author: Luís Costa-Neves – Civil Engineering Department, University of Coimbra – Rua Luís Reis Santos, Polo II FCTUC 3000 Coimbra – Tel.: (351) 239797213– e-mail: luis@dec.uc.pt

# 1 Introduction

In the last few years the use of structural hollow sections had registered a significant increase in their use. These sections are generally used to perform mainly truss structures leading to all their members to be subjected to axial loads. For instance, in Figure 1 presents a truss numerical model of a real structure constituted by hollow sections.

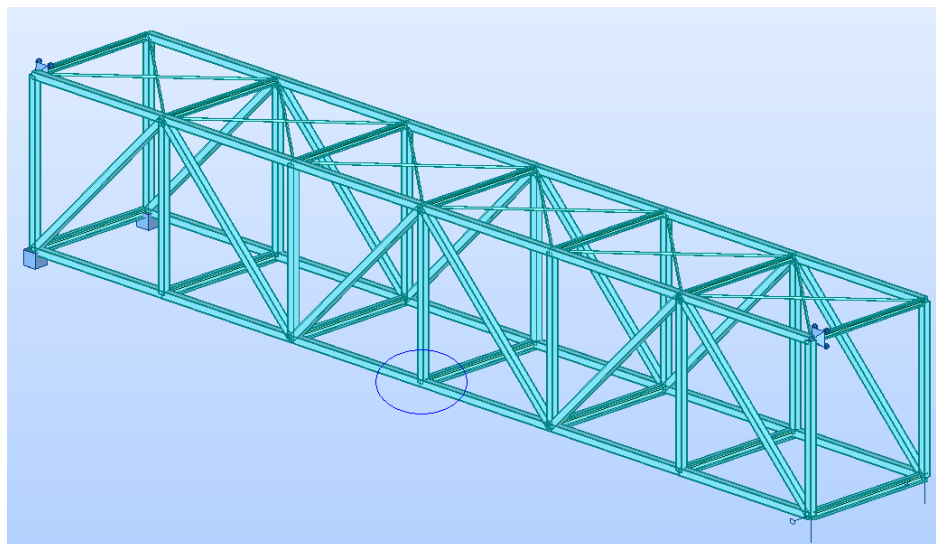


Figure 1: Numerical model of a 3D truss structure

This paper will be focused on "T" connections behaviour which presents the geometry highlighted in Figure 1. The horizontal members of these connections are called chords and the vertical members are called braces.

As the truss structures have all members loaded, this study will be performed with axial loads in the braces and in the chords. The applied load in brace is increased until the connection rupture (tension) while the chord load is considered equal to  $0.5N_{pl}$  and  $0.8N_{pl}$  (for tension and compression).

For instance, in the structure presented in Figure 1, the chord load was 1170.2 kN. For this chord load level the adopted section was 200x200x8 [mm] ( $A=52,9 \text{ cm}^2$ ). Considering an steel grade of 275 MPa this load correspond to  $0.72N_{pl}$  and so, the applied load level of  $0,8N_{pl}$  is a satisfactory.

These connections present a minor axis behaviour characterized by force-displacement ( $F-\delta$ ) or moment-rotation ( $M-\theta$ ) curves described in Figure 2. These curves present an initial stiffness,  $S_{j,ini}$ , and after failure, a membrane stiffness,  $S_{j,m}$  significantly smaller than the first.

The main characteristic of these curves is that there is no point that indicates the failure zone of the connections. This fact motivated the development of approximated methods to evaluate this failure load such as the following.

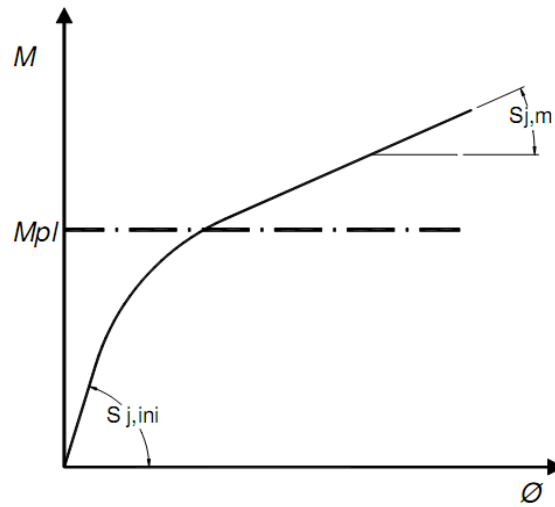
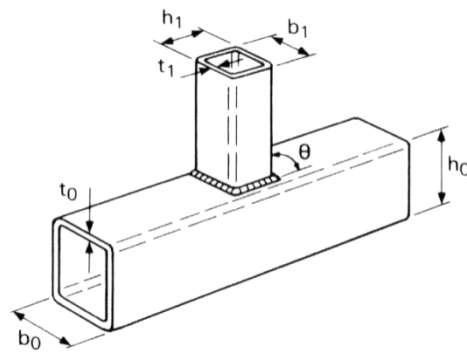


Figure 2: Minor axis moment-rotation curve

This study will be focused in the comparison between numerical results and analytical results obtained using the new recommendations provided by the Eurocode 3, part 1.8 [5]. The main geometric parameters of these "T" connections are presented in Figure 3.



$$\beta = \frac{b_1}{b_0} \quad (1)$$

$$\mu_1 = \frac{b_1}{t_1} \quad (2)$$

$$\mu_0 = \frac{b_0}{t_0} \quad (3)$$

$$\gamma = \frac{b_0}{2t_0} \quad (4)$$

Figure 3: "T" connection with SHS and geometrical parameters

## 2 Bibliographic Review – Chord Axial Load Effect

The main authors who studied this problem were Lu and Wardenier [15], Kostas et al. [10] and Cao et al. [2], [3]. These authors concluded that the tensile axial load in the chord have a positive effect in the connection resistance because this load act like a pre-stress load. These authors also refer that for compression load in the chord the effect is the opposite leading to a reduction of the joint capacity for compression axial loads.

Cao et al. [3] proposed an expression to evaluate the connection resistance when loaded with compression chord axial load. These authors defined a factor  $f(n)$  which is multiplied by the connection resistance expression. This factor assumes a value of 1 for tensile axial load and 1 or less for compressive axial load. The  $f(n)$  factor is nowadays used in the Eurocode 3, part 1.8 [5] with the name of  $k_n$  for connections with  $\beta \leq 0,85$  - see eq. (2).

### 3 Out of Plane Loaded Chord Face Resistance

#### 3.1 Resistance

As it was presented in the Figure 2, the F- $\delta$  curves did not have an explicit point which indicates the failure of the connections. Alternatively, there are some methods used to estimate the load failure with the use of the F- $\delta$  curves.

The first method consists in approximating the F- $\delta$  curve in two tangent straight lines related to the initial stiffness part and to the membrane stiffness part, respectively. The connection failure load is assumed to be present at the intersection of these two lines.

Another available method to estimate the connection resistance consists in defining a maximum displacement for the connection. Some authors proposed values for this displacement. Korol e Mirza [7] proposed a value of 25 times Young Modulus (E) which showed to be similar to  $1.2t_0$  and Lu *et al.* (cited in Koteski *et al.* [10]) who defined a maximum displacement with a value of  $3\%.b_0$ . This deformation limit criteria was also reviewed and accepted by Zhao [19].

This result of  $3\%.b_0$  is nowadays accepted and is also the value used for the International Institute of Welding (IIW) for the maximum displacement for ultimate limit states and  $1\%. b_0$  for service limit states.

The other existing method to estimate the failure load is the rupture line method which is a theoretical method according to Packer *et al.* [17]. These authors developed an optimization mechanism  $\theta$  and were verified by Koteski *et al.* [10] which concluded that the results obtained by Packer *et al.* [17] presented a good agreement for  $\beta \leq 0,7$  while for  $\beta \geq 0,7$ . Considering  $\beta \geq 0,7$  the ultimate limit state may be obtained from a combination of bending and punching shear.

Gomes [6] proposed some mechanisms formed by straight and logarithmic lines and compared these results with Packer *et al.* [17]. He concluded that his results presented a better approach to the connection resistance.

#### 3.2 Initial and Membrane Stiffness

As showed in Figure 2, these connections present two different behaviours. After the connection failure ( $M_{pl}$  in Figure 2) these connections present an initial stiffness with a value of  $S_{j,ini}$  which increases with an increase of  $\beta$ .

Some authors indicate that the connections designers should approximately the value of this parameter by some analytical expressions such as presented by Czechowski *et al.* (cited by Neves [16]).

Before the connection failure there is some reserve of resistance called membrane stiffness with a value of  $S_{j,m}$ . Some analytical approaches were developed to estimate this parameter. Thornton *et al.* (cited Neves [16]) presented an analytical approach for this parameter. This method can be estimate by the connection ultimate load and with the aid of another method presented in the Eurocode 3, part 1.8 [5] that can estimate the connection failure load. The difference between these two methods leads to an estimation of the membrane stiffness.

## 4 Eurocode 3 approach

The Eurocodes were developed in order to homogenise the methodologies applied around the Europe. The steel structures design is made considering the Eurocode 3 and in its part 1.8. The Eurocode 3, part 1.8 [5] consider, for these connections, the failure modes presented in Figure 4.

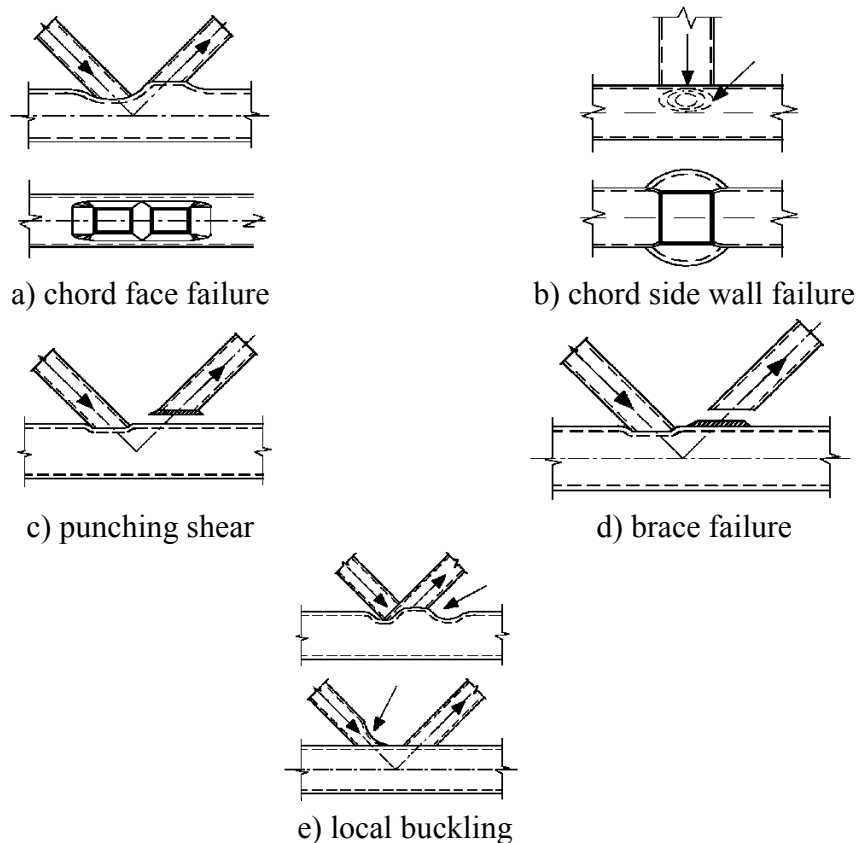


Figure 4: Failure modes (Eurocode [5])

This methodology is applied to the connections who present some requirements like  $\beta \geq 0.25$ ,  $\mu_0 \leq 35$  e  $\mu_1 \leq 35$ , respectively.

The Eurocode 3, part 1.8 [5] only consider, in their expressions, the influence of chord axial load for connections with  $\beta \leq 0.85$  for the ultimate limit state of the chord face plastification. For higher values of  $\beta$  an interpolation between the values of the chord face plastification with  $\beta = 0.85$  and the chord side wall failure for  $\beta = 1$  should

be made. However, for the other failure modes for  $\beta \geq 0.85$  there are no references to the effects of chord axial load.

Equation (1) defines, according to Eurocode 3, part 1.8 [5] the plastic load for the chord face, in the case of the “T” joint using the geometric parameters present in Figure 3.  $N_{i,Rd}$  is the brace axial load leading to the yielding or punching of the chord face. To compute this value, equation (5) from the Eurocode [5] should be used if  $\beta \leq 0,85$ :

$$N_{i,Rd} = \frac{k_n f_{y0} t_0^2}{(1-\beta) \sin \theta_i} \left( \frac{2\eta}{\sin \theta_i} + 4\sqrt{1-\beta} \right) / \gamma_{M5} \quad (1)$$

where  $k_n$  is defined by eq. (2),  $f_{y0}$  is the chord yield stress,  $t_0$  the chord thickness,  $\beta$  is a geometrical parameter defined in Figure 3 and  $\theta_i$  the angle between the chord and the brace.

$$k_n = 1.3 - \frac{0.4n}{\beta} \quad \text{mas } k_n \leq 1.0 \quad (2)$$

## 5 Numerical Simulation

### 5.1 Numerical Model

A finite element model for the studied geometries was developed using four-node thick shell elements, therefore considering bending, shear and membrane deformations. The mesh was more refined near the weld, where the stress concentration is likely to happen, and the more regular as possible, with well proportioned elements to avoid numerical problems.

The material and geometrical properties used in the analysis are presented in Table 1, and are the same used by Lie et al. [12] to calibrate the mechanical model with experiments. It is important to emphasize that the experimental tests performed by Lie *et al.* [12] considered cracked welds. However, in this reference, a numerical result based on the model without cracks in the weld was also presented. These results were used to calibrate the finite element model used in this paper and that will be presented in next sections. The welds were considered as shell elements according to Lee [11] - see Figure 6.

Figure 5 shows the finite element model for the “T” joint, composed of 9482 nodes and 9284 elements performed in the Ansys 10.0 package software [1].

The test layout from Lie et al. [12] is shown in Figure 7. The same layout was reproduced in the numerical model, not only in terms of material properties, but also in terms of the test geometry: span, type of support, load introduction and stiffness near the supports. This was necessary to enable a comparison with the results from [12], in terms of brace load-displacement curves. In fact, this data includes

deformability of the brace itself, of the chord by bending, local chord deformation near the supports, and of course deformations at the connection: chord side walls and chord loaded face deformations.

Table 1 – Mechanical properties after Lie et al. [12].

Specimen	$b_0$ (mm)	$h_0$ (mm)	$t_0$ (mm)	$b_1$ (mm)	$h_1$ (mm)	$t_1$ (mm)	$t_w$ (mm)	$f_y$ (MPa)	$f_u$ (MPa)	$f_w$ (MPa)
T1	350	350	15	200	200	16	12	380.3	529.0	600
T2	350	350	15	200	200	12	12	380.3	529.0	600

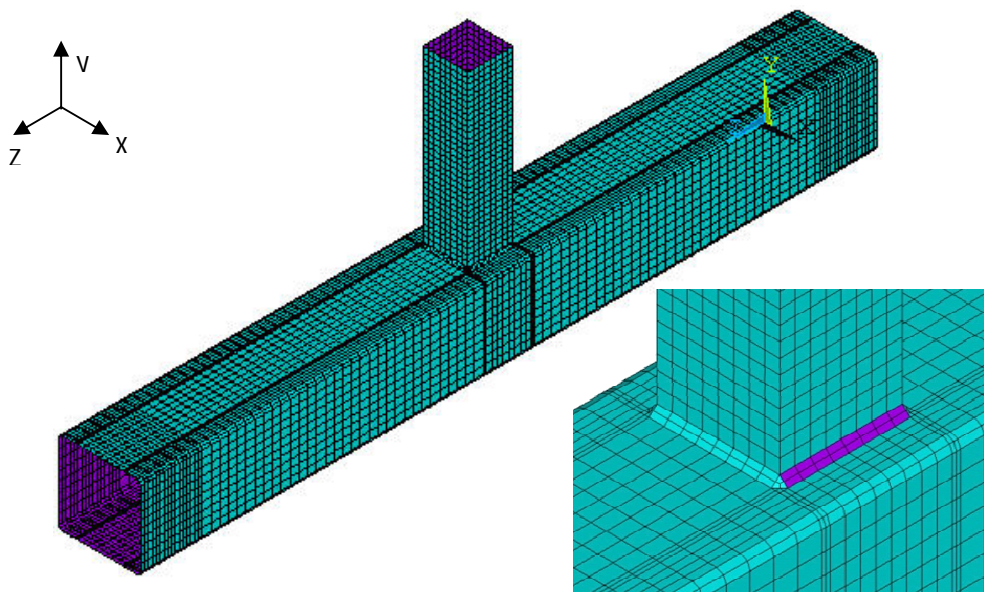


Figure 5: Numerical model

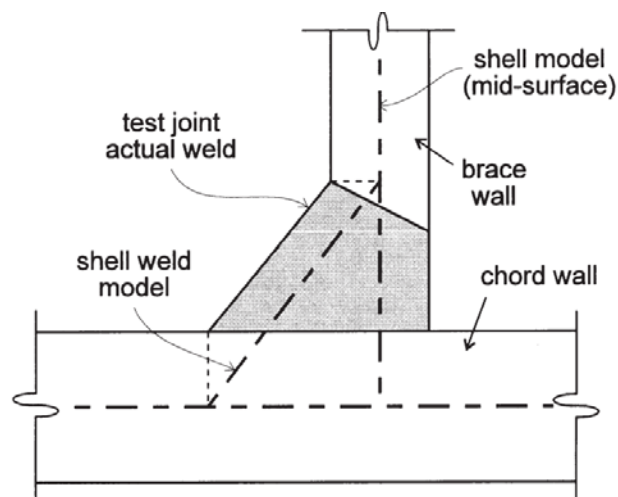


Figure 6: Modelling of the welds by shell elements after Lee [11]

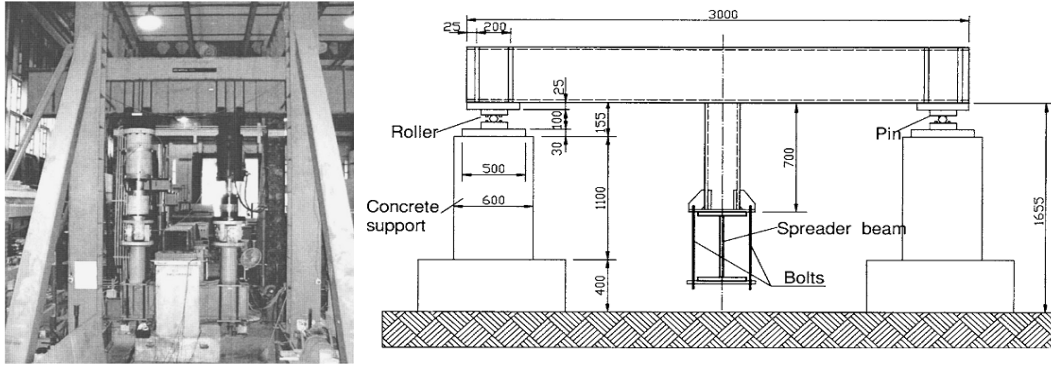


Figure 7: Experimental test layout, after Lie *et al.* [12]

Figure 8 presents the numerical and experimental results where it may be observed a good agreement between these results validating the proposed model. In this figure the Lie *et al.* curve represents the experimental results, Model represents the numerical results, deformation is the value corresponding to a displacement of  $3\%b_0$  and EC3 is the analytical failure load evaluated according to the Eurocode 3, part 1.8 [5].

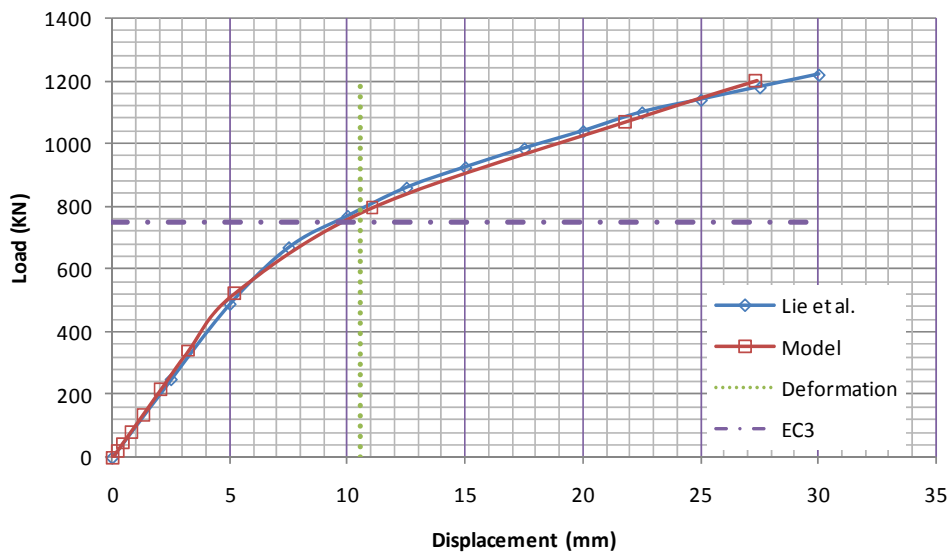


Figure 8: Model validation

The model used in this study was the same presented in the model validation only changing the material properties. In the parametrical analysis performed in this paper a geometric and material (bilinear steel with no strain-hardening) non-linear analysis was adopted. The steel used in the connections members presented a 355 MPa grade and for the welds, a 600 MPa grade was used.

## 5.2 Numerical simulations description

In this study a parametric variation of the connection geometries to determine their influence over the connection behaviour was performed. The performed analyses are presented in Table 2 totalizing 210 simulations. All the parameters used are presented in Table 3.

Table 2: Parametric study

Chord (mm)	Brace (mm)	Brace Force	Chord Force (N/N <sub>pl</sub> )
SHS 300x300xE E=6, 8, 10, 12, 14, 16	SHS 100x100x12 SHS 150x150x12 SHS 180x180x12 SHS 220x220x12 SHS 250x250x12 SHS 260x260x12 SHS 285x285x12	Tension	0 0,5 (Tension) 0,5 (Compression) 0,8 (Tension) 0,8 (Compression)

Table 3: Geometrical parameters

	E6 ( $\gamma=25$ )		E8 ( $\gamma=18.75$ )		E10 ( $\gamma=15$ )		E12 ( $\gamma=12.5$ )		E14 ( $\gamma=10.71$ )		E16 ( $\gamma=9.38$ )	
	t <sub>w</sub>	$\beta$	t <sub>w</sub>	$\beta$	t <sub>w</sub>	$\beta$	t <sub>w</sub>	$\beta$	t <sub>w</sub>	$\beta$	t <sub>w</sub>	$\beta$
M100	12	0.40	12	0.40	12	0.40	12	0.40	12	0.40	12	0.40
M150	12	0.56	12	0.56	12	0.56	12	0.56	12	0.56	12	0.56
M180	12	0.66	12	0.66	12	0.66	12	0.66	12	0.66	12	0.66
M220	12	0.80	12	0.80	12	0.80	12	0.80	12	0.80	12	0.80
M250	12	0.90	12	0.90	12	0.90	12	0.90	12	0.90	12	0.90
M260	12	0.93	12	0.93	12	0.93	12	0.93	12	0.93	12	0.93
M285	10	1.00	8	0.99	6	0.98	6	0.98	5	0.98	4	0.97

The designation E refers to the chord thickness (mm) and the designation M refers to the brace height (mm). The designation used for the loads are BTC0: tension in brace and no force in chord; BTC0.5T: tension in brace and tension of  $0.5N_{pl}$  in chord; BTC0.5C: tension in brace and compression of  $0.5N_{pl}$  in chord; BTC0.8T: tension in brace and tension of  $0.8N_{pl}$  in chord and BTC0.8C: tension in brace and compression of  $0.8N_{pl}$  in chord. The brace height value, adopted for determining of the  $\beta$  value, was calculated using the height of the member plus the double of the effective weld length ( $0.8t_w$ ).

## 6 Results

Figure 9 presents the connection deformed shape corresponding to a chord of 300x300x10 [mm] and brace of 180x180x12 [mm] with a chord tensile load of  $0.5N_{pl}$ . As it can be observed, the main deformation observed in the connection is located in the chord face failure as it was expected since this connection has  $\beta=0.66$  and as described in EC3, this value of  $\beta$  is conditioned for the ultimate limit state of chord face failure.

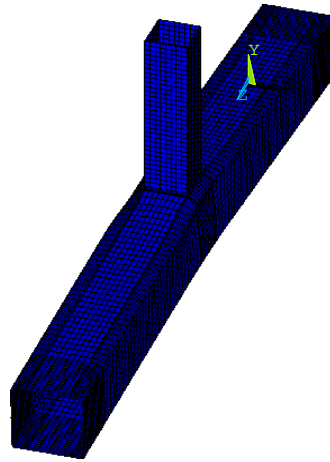


Figure 9: Deformed mesh

Two different analysis were considered to perform a parametric analysis with chord axial loads. The first step considers only the chord load and the second step adds the brace load effect. Figure 10 presents the *Von Mises* stress distribution after the application of chord axial load and after the connection failure with the application of brace load. As it can be observed in Figure 10(a) the load stresses obtained in the chord have, as expected, a value of about 0.5 times the yield stress (355 MPa). Figure 11 presents the stresses according to the directions X, Y e Z respectively.

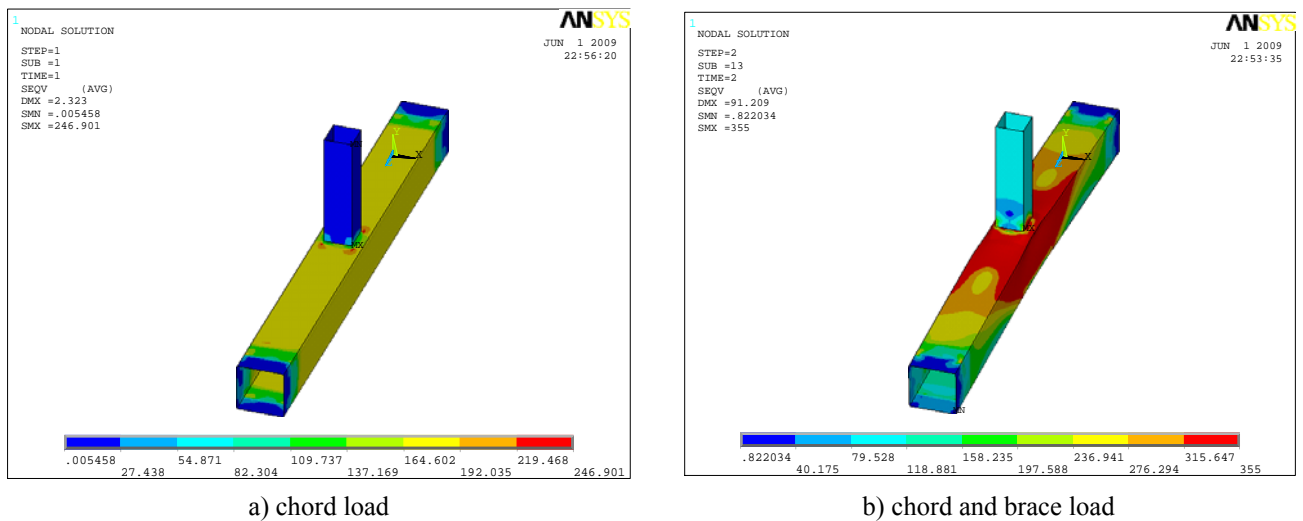
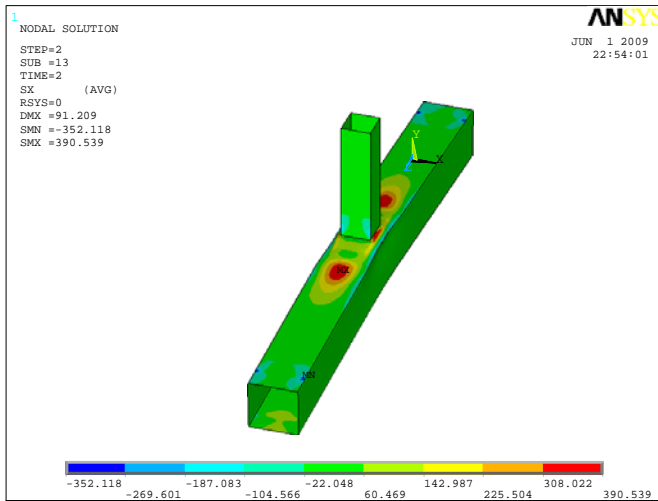
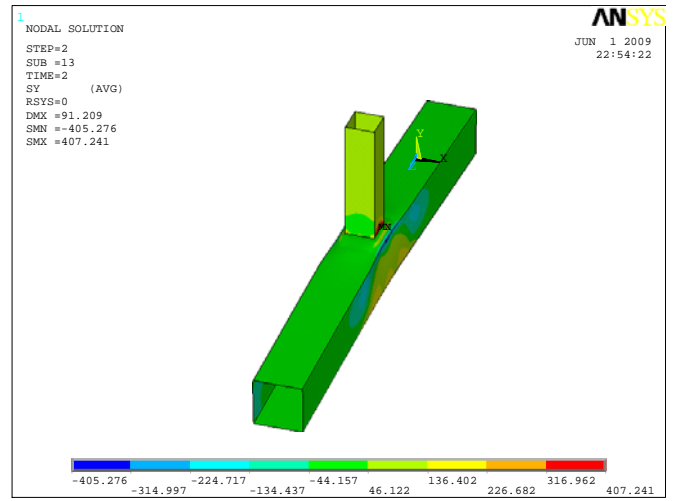


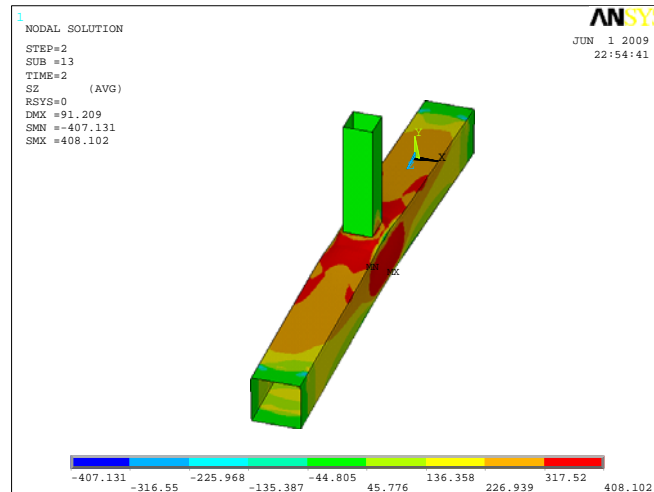
Figure 10: Von Mises stress distribution



a) X direction stress



b) Y direction stress

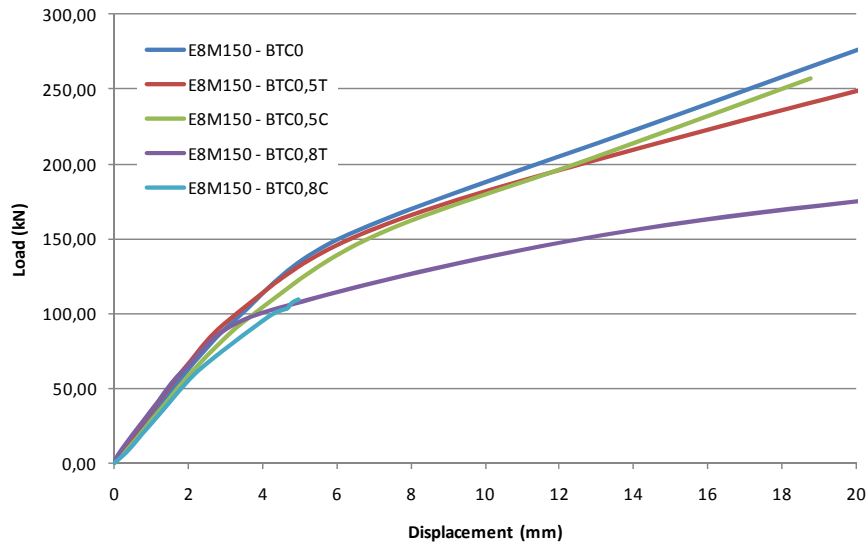


c) Z direction stress

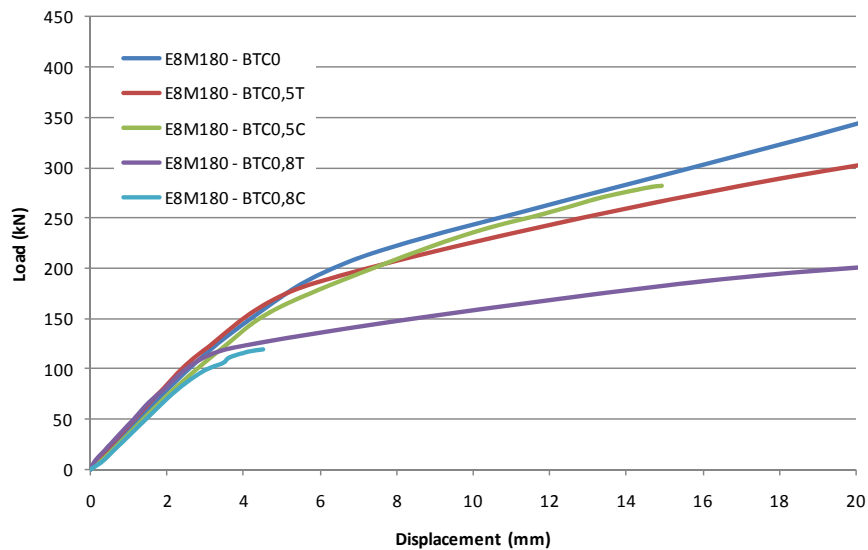
Figure 11: Normal stresses distribution

The  $F-\delta$  curves presented in Figure 12 were obtained in the numerical simulations, with a constant value of  $\gamma$  considering all chord loads cases according to Table 2. This paper will only present the results related to a chord thickness of 8 mm and brace heights of 150 and 180 mm.

The curves presented in Figure 12 have a shape similar to the curve showed in the Figure 2 considering a minor axis connection behaviour. The case without chord load is the situation with the highest connection resistance. In the case of chord with tension loads, the ultimate connection load is larger then the case with compression chord loads. The present study also enable a comparison of cases with different chord loads levels. The numerical resistance was obtained with the out of plane chord maximum displacement of  $3\% \cdot b_0$  (9 mm).



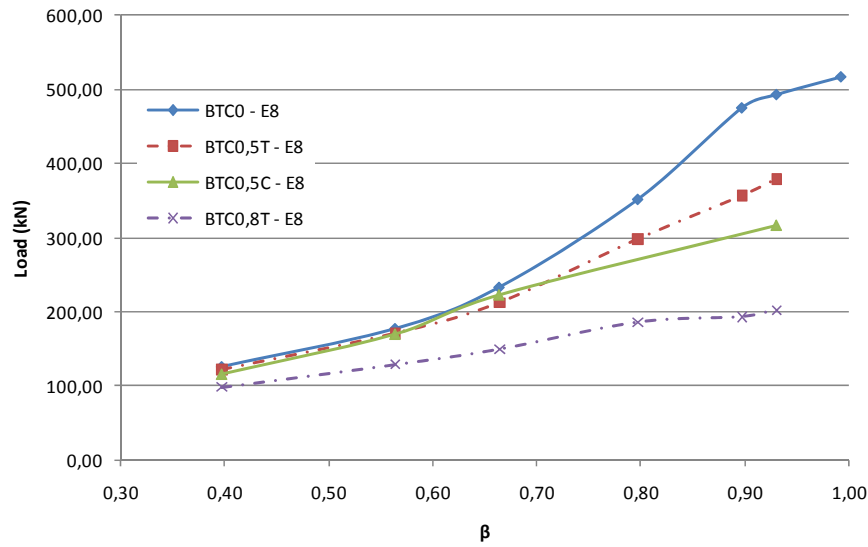
a) brace height of 150 mm



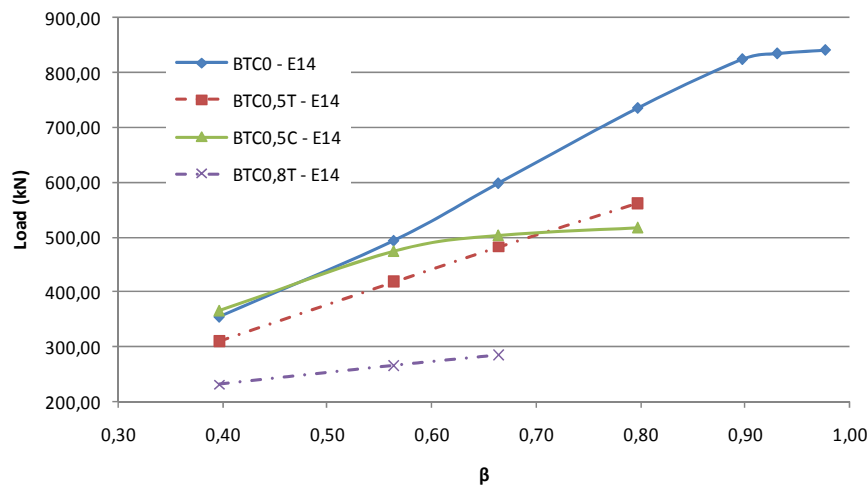
b) brace height of 180 mm

Figure 12: F- $\delta$  curves – influence of axial load

In spite of the chord load type, the connection resistance increase with the increase of  $\beta$  according to Figure 13. For  $\beta \leq 0.7$  the effect of tension load in the chord increase the connection resistant when compared with compression load in the chord for the same value of  $\beta$ . For higher tension chord loads ( $0.8N_{pl}$ ), the connections resistance were smaller than the other loads (tension and compression).



a) chord thickness = 8mm



b) chord thickness = 14mm

Figure 13: Numerical resistance – influence of axial load

Table 4 presents a comparison between the numerical and the analytical resistance according to chord load level variation. The results presented in Table 4 shows that, for low values of  $\beta$  ( $\beta \leq 0.8$ ) there is a good agreement between the numerical and analytical values. The difference between the two methods increase with an increase of the chord thickness. For higher values of  $\beta$  ( $\beta \geq 0.8$ ) the difference between the two methods is very high for any chord loading. This is practically due to the predominance of chord face failure. The situations with chord tension load present results larger differences between analytical and numerical results than for the compression cases with the same load intensity. Figure 14 presents results comparing the initial stiffness for different load cases.

Table 4: Numerical and analytical approach

		N=0		N=0,5.N <sub>pl</sub>		N=-0,5.N <sub>pl</sub>		N=0,8.N <sub>pl</sub>		N=-0,8.N <sub>pl</sub>	
		Num.	EC3	Num.	EC3	Num.	EC3	Num.	EC3	Num.	EC3
E8	M100	125.89	142.2	122.21	142.2	115.35	113.3	98.67	142.2	-	70.3
	M150	177.21	189.7	171.35	189.7	169.52	179.4	129.08	189.7	-	139.0
	M180	233.03	237.9	212.55	237.9	222.77	237.6	149.69	237.9	-	194.6
	M220	351.76	366.3	298.18	366.3	-	366.3	185.71	366.3	-	329.2
	M250	475.26	853.2	356.66	853.2	-	853.2	193.12	853.2	-	834.3
	M260	493.32	1080.0	379.17	1080.0	317.04	1080.0	202.44	1080.0	-	1080.0
	M285 (tw=8)	517.27	1781.3	-	1781.3	-	1781.3	-	1781.3	-	1780.7
E14	M100	353.45	435.5	310.92	435.5	365.97	346.9	230.55	435.5	-	215.4
	M150	492.37	581.1	418.33	581.1	474.29	549.4	265.04	581.1	-	425.7
	M180	597.09	728.6	482.11	728.6	503.07	727.8	284.23	728.6	-	596.1
	M220	734.39	1121.8	562.33	1121.8	517.19	1121.8	-	1121.8	-	1008.1
	M250	823.46	2024.7	-	2024.7	-	2024.7	-	2024.7	-	1966.9
	M260	833.92	2467.8	-	2467.8	-	2467.8	-	2467.8	-	2437.0
	M285 (tw=6)	840.26	3297.3	-	3297.3	-	3297.3	-	3297.3	-	3292.3

The results also indicated a initial stiffness value increase, for each load case, with the increase of  $\beta$ . In Figure 14 it can be observed that tensile chord loads have a favourable influence over the initial stiffness when compared with the case without chord axial loads or even chord compression loads. The cases with smaller values of chord load s( $0.5N_{pl}$ ), under tension or compression, produce more accurate results for initial stiffness than the cases with a higher chord loads.

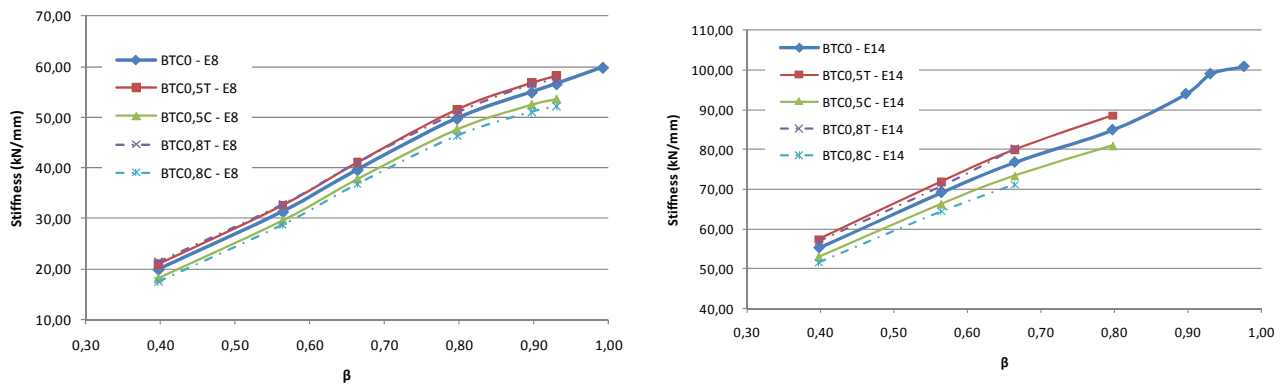


Figure 14: Initial stiffness – influence of chord loading

## 7 Conclusions

As it can be seen in Figure 8, the numerical model was properly validated against experimental results. The results indicated that the resistance and the initial stiffness of the connection increase with the increase of  $\beta$  as it was previously observed by several authors.

The case without chord axial loads is the situation where the higher connection resistance was reached as can be observed in Figure 13. For  $\beta \leq 0.7$  the case of compressive chord axial loads led to more accurate resistance results while the opposite occurs for higher values of  $\beta$ . The case of high tensile chord loads was the most severe of all investigated cases.

According to EC3 approach this shouldn't happen because the tensile chord load do not affect the connection resistance and that wasn't observed in this study, so a review of this approach is advised, namely the  $k_n$  factor.

The comparison between the numerical and analytical resistances shows that, for cases where the chord face failure is dominant, the results are very similar, however for the cases where the other modes govern, the differences are still significant so it is important to review of this expressions or the validity of the  $3\% \cdot b_0$  as the maximum displacement for this values of  $\beta$ .

As the tensile chord load act like a pre-stress load, it tends to increase the initial stiffness of the connection when compared with the other load cases as it was observed in Figure 14. For higher chord loads (tension and compression), the initial stiffness tends to decrease because this load value is already close to the connection failure.

## References

- [1] Ansys 10.0 ®, ANSYS – Inc. Theory Reference, 2005.
- [2] J.J. Cao, J.A. Packer, N. Kosteski, “Determination of connection strength between longitudinal plates and RHS columns”, Journal of Constructional Steel Research, vol. 46: 1-3, paper n°134, 1998.
- [3] J.J. Cao, J.A. Packer, G.J. Yang, “Yield line analysis of RHS connections with axial loads”, Journal of Constructional Steel Research, vol. 48, n°1, pp 1-25, 1998.
- [4] EUROCODE 3. EN 1993-1-1, Design of steel structures Part 1.1: General rules and rules for buildings, Brussels, CEN-European Committee for Standardisation, 2005.
- [5] EUROCODE 3. EN 1993-1-8, Design of steel structures Part 1.8: Design of joints, Brussels, CEN-European Committee for Standardisation, 2005.
- [6] F.C.T. Gomes, F.C.T., “Etat limite ultime de la résistance de l'âme d'une colonne dans un assemblage semi-rigide d'axe faible”, Rapport Interne n° 203, MSM – Université de Liège, 1990.
- [7] R. Korol, F. Mirza, “Finite element analysis of RHS T-joints”, Journal of the Structural Division, ASCE, vol. 108, No.ST9, pp. 2081-2098, 1982.
- [8] N. Kosteski, J.A. Packer, “Bracing connections to rectangular HSS columns”, Connections in Steel Structures IV – Behaviour Strength and Design, Proceedings Fourth International Workshop Oct 2000, Roanoke, Virginia, USA, AISC/ECCS, 2002, pp 788-797, 2000.
- [9] N. Kosteski, J.A. Packer, “Welded Tee-to-HSS connections”, Journal of Structural Engineering, vol. 129, n°2, pp 151-159, 2003.

- [10] N. Kostasiki, J.A. Packer, R.S. Puthli, “A finite element method based yield load determination procedure for hollow structural section connections”, *Journal of Constructional Steel Research*, vol. 59, pp 453-471, 2003.
- [11] M.M.K. Lee, “Strength, stress and fracture analyses of offshore tubular joints using finite elements”, *Journal of Constructional Steel Research*, vol. 51, pp 265-286, 1999.
- [12] S. Lie, S. Chiew, C. Lee, Z. Yang, “Static strength of cracked square hollow section T joints under axial loads. I: Experimental”, *Journal of Structural Engineering*, vol. 132, nº 3, pp 368-377, 2006.
- [13] L.R.O. Lima, L.F.C. Neves, J.G.S. Silva, P.C.G.S. Vellasco, “Análise paramétrica de ligações “T” com perfis tubulares em aço através de um modelo de elementos finitos”, *Proceedings of the XXVI Iberian Latin-American Congresso n Computational Methods in Engineering – CILAMCE, Brazilian Assoc. for Comp. Mechanics (ABMEC) & Latin-American Assoc. of Comp. Methods in Engineering (AMC), Guarapari, Espírito Santo, Brazil, 19<sup>th</sup>-21<sup>st</sup> October 2005*, 2005.
- [14] L.R.O. Lima, L.F.C. Neves, J.G.S. Silva, P.C.G.S. Vellasco, S.A.L. Andrade, “Parametric Analysis of RHS T Joints Under Static Loading”, *CC2007 - 11th International Conference on Civil, Structural and Environmental Engineering Computing, Saint Julians, Proceedings of the 9th International Conference on the Application of Artificial Intelligence to Civil, Structural and Environmental Engineering, Edimburg, Civil Comp Press v.1. p.1-15*, 2007.
- [15] L.H. Lu, J. Wardenier, “The ultimate mean strength of I-beam to RHS column connections”, *Journal of Constructional Steel Research*, vol. 46: 1-3, paper nº 139, 1998.
- [16] L.F.C. Neves, “Comportamento monotónico e cíclico de ligações de eixo fraco e tubulares em estruturas metálicas e mistas aço-betão”, PhD, University of Coimbra, 2004.
- [17] J. Packer, G. Morris, G. Davies, “A limit states design method for welded tension connections to I-section webs”, *Journal of Constructional Steel Research*, vol.12, pp 33-53, 1989.
- [18] X. Zhao, G. Hancock, “Plastic Mechanism analysis of T-joints in RHS subject to combined bending and concentrated force”, *Proceedings of the Fifth International Symposium on Tubular Connections held at Nottingham, UK, August 1993, E & FN Spon, London, pp 345-352*, 1993.
- [19] X. Zhao, “Deformation limit and ultimate strength of welded T-joints in cold-formed RHS sections”, *Journal of Constructional Steel Research*, vol. 53, pp 149-165, 2000.